Journal of Energy Chemistry 36 (2019) 122–128

Contents lists available at ScienceDirect

Journal of Energy Chemistry

journal homepage: www.elsevier.com/locate/jechem

http://www.journals.elsevier.com/journal-of-energy-chemistry/

Highly selective adsorption of CO over N_2 on CuCl-loaded SAPO-34 adsorbent

Yaqi Wu[a,b], Zhaoan Chen[a], Bing Li[a], Jiacheng Xing[a,b], Hanbang Liu[a,b], Yansi Tong[a,b], Peng Tian[a], Yunpeng Xu[a,*], Zhongmin Liu[a,*]

[a] Dalian National Laboratory for Clean Energy, Dalian Institute of Chemical Physics, Chinese Academy of Sciences, Dalian 116023, Liaoning, China
[b] University of Chinese Academy of Sciences, Beijing 100049, China

Dedicated to the 70th anniversary of Dalian Institute of Chemical Physics, CAS, China.

ARTICLE INFO

Article history:
Received 5 June 2019
Revised 26 July 2019
Accepted 26 July 2019
Available online 30 July 2019

Keywords:
CO/N_2 separation
SAPO-34
CuCl
π complexation

ABSTRACT

Carbon monoxide (CO)/N_2 separation is of importance for current chemical industry. However, CO/N_2 separation remains a challenge due to the similar molecular size and the small variance of volatility of CO and N_2. In this work, molecular sieve SAPO-34 was loaded with CuCl by monolayer dispersion method for the preparation of Cu(I) containing adsorbents. The resulted adsorbents were characterized via nitrogen adsorption/desorption at 77 K, X-ray fluorescence (XRF) and X-ray diffraction (XRD). The results indicated that CuCl was successful loaded into the molecular sieve and well-dispersed. CO and N_2 single component adsorption isotherms were recorded under 298 K, 308 K and 318 K by using volumetric method. One of the CuCl-loaded SAPO-34 adsorbent exhibited a very high CO adsorption capacity of 1.84 mmol/g at 100 kPa, 298 K and high CO/N_2 selectivity.

Zhongmin Liu was born in Henan Province on Sept 24, 1964. He received his BS degree in Physical Chemistry from Zhengzhou University in 1983 and his Ph.D. in Physical Chemistry from Dalian Institute of Chemical Physics in 1990. He has been the Director of Dalian Institute of Chemical Physics, CAS since 2017. In 2006 Prof. Liu and his colleagues successfully demonstrated industrial methanol-to-olefins (DMTO) technology. Based on this, the world's first commercial MTO unit was built by the Shenhua group, which is a milestone in the field of coal to chemicals. Besides DMTO, Prof. Liu has also developed many other new catalysts and catalytic processes, such as methanol to ethanol, propylene to isopropanol and methanol to dimethyl ether. Recently, the world's first Coal-to-Ethanol (methanol to ethanol) demonstration plant (100 KTA ethanol) was commissioned.

Yunpeng Xu, was born in 1973 in Dalian, Liaoning Province. He graduated from Peking University in 1996 and received his BS degree in Physical Chemistry. In 2001, he received his Ph.D. degree in Physical Chemistry from Dalian Institute of Chemical Physics (DICP), Chinese Academy of Sciences, under the supervision of Prof. Liwu Lin. He was promoted to Full Professor of DICP in 2009. He is dedicated to the development of catalysts and new catalytic processes. His current research interests include synthesis of molecular sieves and development of adsorbents. He has authored more than 60 scientific publications and 80 patents.

1. Introduction

Carbon monoxide (CO) is a critical raw material for the synthesis of varieties of basic chemicals ranging from methanol, acetic acid, polyurethanes to phosgene, etc. [1]. Furthermore, with the rapid development of C1 chemistry, CO becomes more and more important [2]. Generally, a very large amount of low-cost CO primarily existed in the off gas streams from many industrial processes, such as tail gas in yellow phosphorus production, carbon black tail gas and coke oven/blast furnace gas [3]. However, in these gas streams, CO always mixed with a certain amount of

* Corresponding authors.
E-mail addresses: xuyp@dicp.ac.cn (Y. Xu), liuzm@dicp.ac.cn (Z. Liu).

https://doi.org/10.1016/j.jechem.2019.07.013

N_2. Therefore, it is of great importance for the separation and purification of CO/N_2.

At present, the three most commonly used methods for the separation of CO/N_2 are cryogenic distillation, membranes and adsorption [4–6]. Because of the low-energy consumption, high efficiency and easy operation, adsorption has gain plenty of attentions for CO separation and purification. Cu(I) containing adsorbents has been widely used and proved to be very effective for preferentially adsorb CO over N_2 due to the formation of strong π complexation bonds between Cu(I) ion and CO. Many porous materials have been used as support to load Cu(I) ions, including molecular sieves, activated carbons and metal organic frameworks (MOFs) [3,6–9]. Molecular sieve is one of the most valuable adsorbents for industrial applications due to their high stability, low cost and easily synthesis processes. The conventional CO molecular sieve adsorbents are Si-Al zeolites often incorporated with Cu(I) or Ag(I) which have been developed for decades and the types of utilized zeolites were limited. Thus, developing new molecular sieve adsorbents for CO separation will be no doubt of significance.

Silicoaluminophosphate molecular sieves (SAPO) are a significant class of inorganic crystalline porous materials. Among them, SAPO-34 has attracted worldwide attention due to its successful industrial application in methanol to olefins (MTO). However, the current application of SAPO-34 is mainly focused on MTO reaction [10–12], NO_x reduction [13,14] and CO_2/CH_4, N_2/CH_4 separation as membranes [15–18] while applications in other fields were rarely reported. In present work, for the first time, we found that silicoaluminophosphate molecular sieve, SAPO-34, also can be potential adsorbent support for CO separation. We have synthesized a series of SAPO-34 adsorbents incorporated with different loading of CuCl through a monolayer dispersion method. The resulting samples were characterized via N_2 adsorption/desorption at 77 K, X-ray fluorescence (XRF) and X-ray powder diffraction (XRD) and were tested for single component adsorption of CO and N_2 under different temperatures. Furthermore, isosteric heat of CO and N_2 adsorption on the resulting samples were analyzed by fitting the adsorption isotherms with Langmuir–Freundlich model and then calculated using Clausius–Clapeyron equation in order to clarify the adsorption mechanism.

2. Experimental

2.1. Materials

SAPO-34 templated by tetraethylammonium hydroxide (TEAOH) was synthesized with a starting gel composition of $2.0TEAOH/1.0Al_2O_3/1.0P_2O_5/0.2SiO_2/60H_2O$ at 473 K for 8 h via hydrothermal methods. The as-synthesized materials were calcined in air at 873 K for 4 h to remove the occluded organic structure-directing-agents. CuCl (97%) was purchased from Acros. The purity of N_2 and CO were all 99.999%.

2.2. Preparation of SAPO-34/CuCl adsorbents

A certain amount of SAPO-34 powder and CuCl were mixed together and grinded fully under anhydrous and anaerobic conditions. Then, the mixture was placed in a quartz tube for the calcination temperature of 723 K for 4 h under N_2 atmosphere (120 mL/min). For the copper loadings of 0.1, 0.3, 0.4, 0.5 and 0.6 g/g SAPO-34, the samples were denominated as SCu(X), where X is the copper loadings in grams per gram SAPO-34.

2.3. Characterizations

The X-ray diffraction (XRD) patterns were collected on a PANalytical X'Pert PRO X-ray diffractometer using the Cu-$K\alpha$ radiation ($\lambda = 1.54059$ Å), operating at 40 kV and 40 mA. The Cu content of the adsorbents were determined by X-ray fluorescence (XRF) (PANalytical Axios advanced). N_2 adsorption-desorption isotherms of the samples were measured at 77 K on a Micromeritics Gemini VII 2390 system. The specific surface areas were calculated from the isotherms based on Brunauer–Emmett–Teller (BET) equation from the data on N_2 adsorption isotherm. The total pore volumes were estimated to be the liquid volume of N_2 at a relative pressure (p/p_0) of 0.98 from the adsorption equilibrium isotherms.

2.4. Adsorption measurement

Both single component adsorption of CO and N_2 on the resulting adsorbents were performed by volumetric methods in a Micromeritics Gemini VII 2390 adsorption apparatus. CO and N_2 adsorption isotherms were measured at varied temperatures (298 K, 308 K and 318 K) and up to atmospheric pressure (~102 kPa). A Dewar with a circulating jacket connected to a thermostatic water bath was used to strictly control the measuring temperatures. The free space of the system was determined by dozing helium gas. The CO and N_2 with high purity of 99.999% were used without further purification.

2.5. Adsorption theories

From the adsorption equilibrium isotherms, many useful information can be obtained, such as the interactions between the adsorbate and adsorbent, the surface information of the adsorbents. In this work, Langmuir–Freundlich model was applied to fit the pure adsorption isotherms of CO and N_2 on the CuCl-loaded SAPO-34 adsorbents [19], which can be expressed as Eq. (1).

$$q = q_m b p^{\frac{1}{n}} / \left(1 + b p^{\frac{1}{n}}\right) \quad (1)$$

where q is the amount adsorbed in equilibrium (mmol/g), q_m is the amount adsorbed at saturation (mmol/g), p is the bulk gas pressure in equilibrium (kPa), b is the adsorption equilibrium constant and n is a model constant.

2.6. Isosteric heat of adsorption

The isosteric heat of CO and N_2 adsorption were calculated using Clausius–Clapeyron equation along with Langmuir–Freundlich model based on the data collected from the adsorption equilibrium isotherms at varied temperatures. The Clausius–Clapeyron equation can be expressed as Eq. (2).

$$(\ln P)_n = -\frac{Q_{st}}{RT} + C \quad (2)$$

Where Q_{st} is the isosteric heat of adsorption (kJ/mol), n is the amount adsorbed (mmol/g), P is the pressure (kPa), R is the universal gas constant (J mol^{-1} K^{-1}), T is the absolute temperature (K) and C is a constant. Thus, the isosteric heat of adsorption Q_{st} was subsequently obtained from the slope of plots of $(\ln P)_n$ as a function of $1/T$.

3. Results and discussion

3.1. Characterizations of the adsorbents

We synthesized a series of SAPO-34-based adsorbents with different CuCl loadings. Fig. 1 shows the N_2 adsorption-desorption isotherms of SAPO-34 and CuCl loaded SAPO-34 adsorbents. Typical type-I isotherms were observed for all the adsorbents, suggesting the microporous properties of the adsorbents. It was noted that the equilibrium adsorbed amount of N_2 decreased with the increase of CuCl loadings. Table 1 listed the normal Cu content

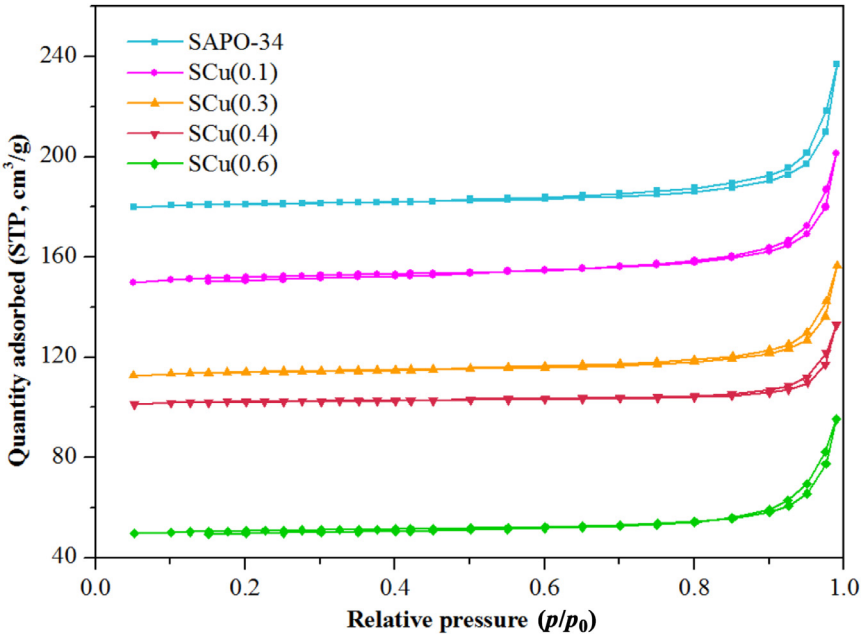

Fig. 1. N_2 adsorption-desorption isotherms of SAPO-34 and CuCl loaded SAPO-34 adsorbents.

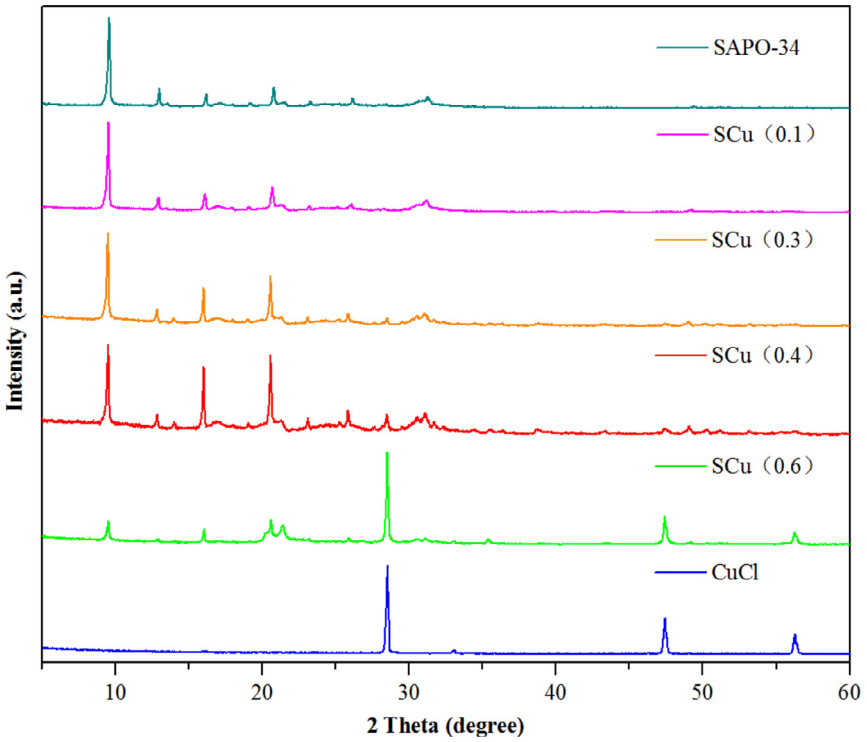

Fig. 2. XRD patterns of SAPO-34 and CuCl loaded SAPO-34 adsorbents.

Table 1. Cu contents and textural properties of SAPO-34 and CuCl loaded SAPO-34.

Samples	Normal Cu content (wt%)[a]	Cu content (wt%)[b]	BET surface area (m^2/g)	Total pore volume (cm^3/g)	Average pore diameter (nm)
SAPO-34	/	/	573	0.32	2.27
SCu(0.1)	5.83	5.89	481	0.28	2.31
SCu(0.3)	14.82	12.36	361	0.21	2.33
SCu(0.4)	18.32	15.12	323	0.18	2.24
SCu(0.6)	24.05	19.29	161	0.12	2.99

[a] Calculated from designed compositions.
[b] Measured by XRF.

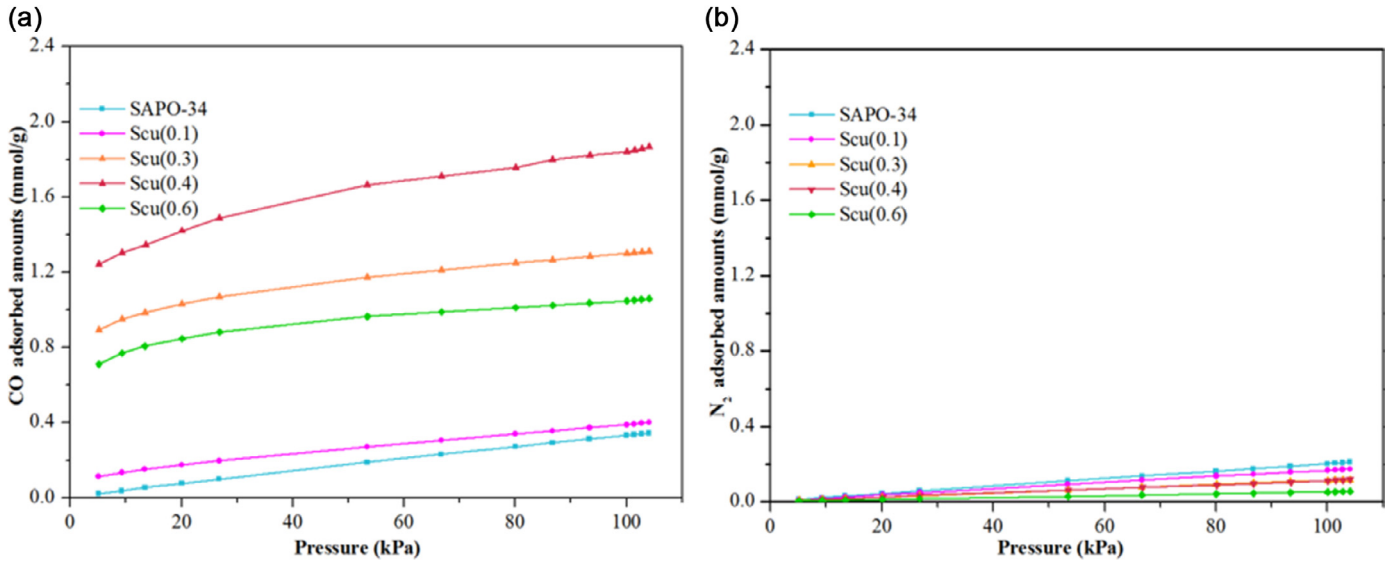

Fig. 3. (a) CO and (b) N_2 adsorption isotherms of SAPO-34 and CuCl loaded SAPO-34 adsorbents at 298 K.

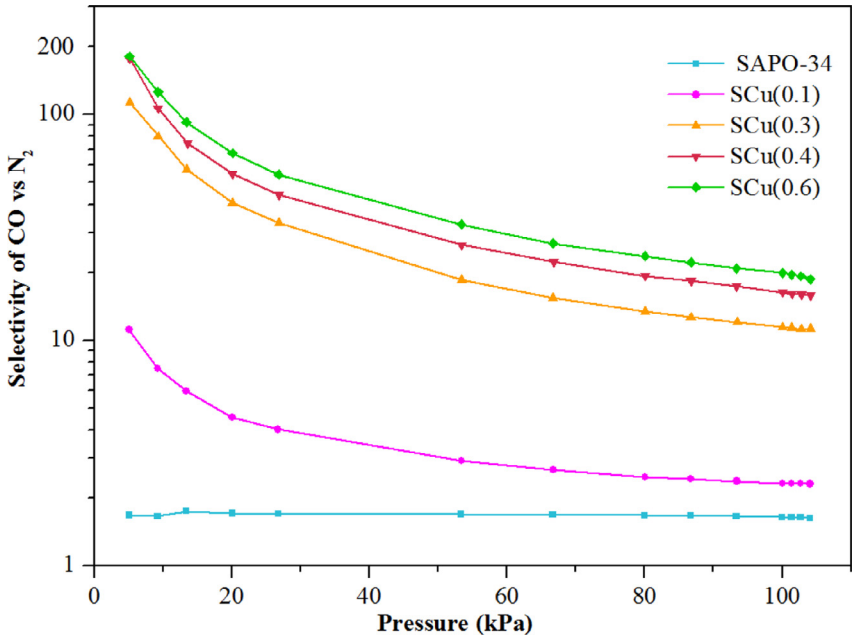

Fig. 4. Equilibrium selectivities of CO/N_2 on SAPO-34 and CuCl loaded SAPO-34 adsorbents at 298 K.

and practical Cu content of SAPO-34 and CuCl loaded SAPO-34 adsorbents measured by XRF. With the increasing loading of CuCl, the discrepancies between measured Cu contents and those used in the materials became obvious. It might be due to the partially collapse of the SAPO-34 framework with the introduction of large amount CuCl which was also in accordance with the XRD results. The BET surface areas, total pore volume and average pore diameter of the resulted adsorbents were also summarized in Table 1. With the increment in CuCl loadings, significant declines in the BET surface area and total pore volume while slightly increases of the average pore diameter were observed. The loading of CuCl has reduced the surface areas and pore volumes of SAPO-34 to a large extent. The more CuCl loadings, the more decreases in the surface areas of SAPO-34.

Fig. 2 shows the XRD patterns of CuCl, SAPO-34 and CuCl-loaded SAPO-34. It can be seen that the crystalline structure of SAPO-34 were well maintained after the loading of CuCl. While with the increase loading of CuCl, the crystallinity of SAPO-34 decreased a lot. No characteristic peaks of CuCl can be observed in the sample SCu(0.1) and a very small peak at 28° matched with CuCl can be seen in sample SCu(0.3) and SCu(0.4), suggesting that CuCl were highly dispersed on the surface of SAPO-34 and the crystallites of CuCl are too small to be detected by XRD. For SCu(0.6), excessive CuCl amounts on the molecular sieve could not be dispersed as monolayer on the surfaces of SAPO-34. Therefore, characteristic diffraction peaks of CuCl were observed in SCu(0.6) and S_{BET} decreased sharply.

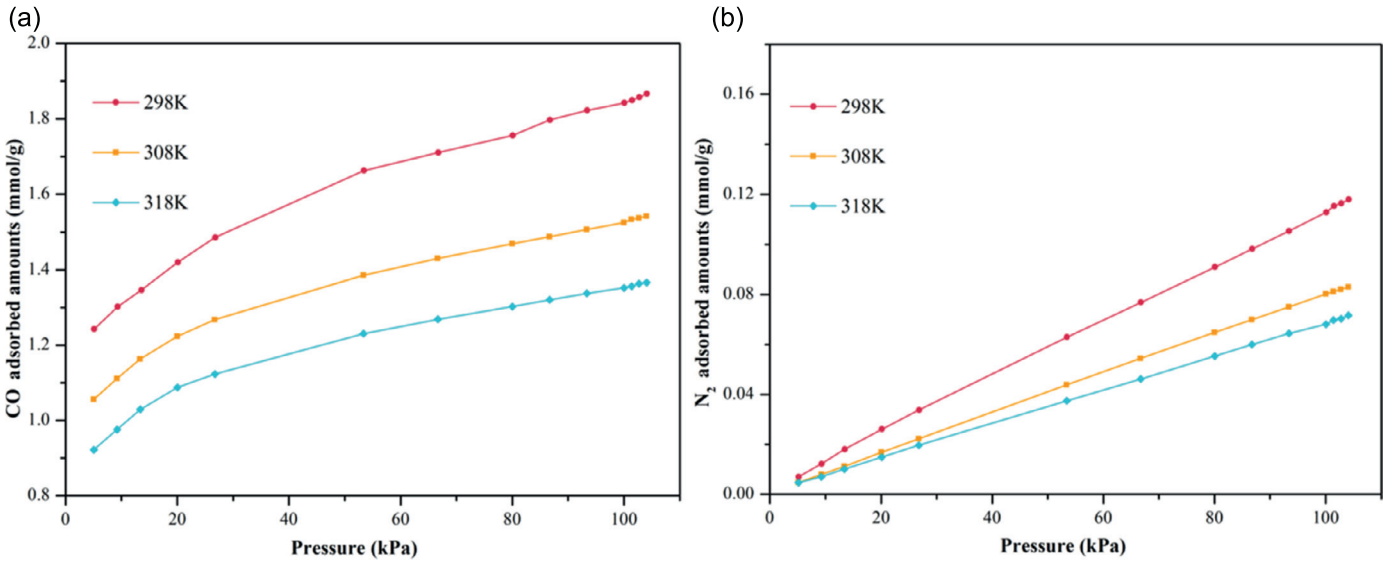

Fig. 5. (a) CO and (b) N_2 adsorption isotherms of SCu(0.4) at 298 K, 308 K and 318 K.

Table 2. Comparison of CO adsorption capacities and CO/N_2 equilibrium selectivities with adsorbents in the literature.

Adsorbent	CO adsorption capacity (mmol/g)	CO/N_2 equilibrium selectivity	Temperature (K)	Ref.
Cu_2O-SBA-15	0.77	6.7	298	[20]
CuCl/AC	~2.45	24	298	[21]
CuCl/Y	2.72	68	303	[6]
AC	0.51	1.6	303	[22]
13X	~0.65	2.7	298	[23]
0.8Cu(I)@MIL-100(Fe)	2.78	18	298	[3]
Cu-BTC	~0.65	3.2	295	[24]
SCu(0.4)	1.84	20	298	This work

3.2. Adsorption performances of the adsorbents

Fig. 3(a) and (b) shows the pure CO and N_2 adsorption equilibrium isotherms at 298 K, respectively. Pure SAPO-34 exhibits similar adsorption amounts of CO and N_2 and the isotherms are near to linear, indicating the weak interactions between SAPO-34 and the gases. With CuCl introduced into SAPO-34, the adsorbed amount of CO increased greatly due to the π-complexation between Cu^+ ions and CO molecules. The CO adsorption isotherms tend to be type-I isotherms, revealing the strong interaction between CO and the adsorbents. It can be seen that with the increment in CuCl loadings, the CO adsorption amount of SCu(0.1), SCu(0.3) and SCu(0.4) increased gradually, which from 0.39 mmol/g of SCu(0.1), 1.30 mmol/g of SCu(0.3) to 1.84 mmol/g of SCu(0.4) at 100 kPa and 298 K. While with further increasing of Cu loadings to 0.6 g/g SAPO-34, the CO adsorption capacity decreased sharply to 1.04 mmol/g at 100 kPa and 298 K which could be attributed to the decreases of surface areas and pore volume caused by the excessive loading and accumulation of CuCl in the molecular sieve. Different from CO adsorption, the interactions between N_2 molecules and the surface of the CuCl loaded SAPO-34 were van der Waals interactions, which N_2 uptake of CuCl-loaded SAPO-34 adsorbents decreased with the loading of CuCl due to the decrease of surface areas and the physical adsorption sites of N_2.

For CO/N_2 separation, besides adsorption capacity, the adsorption selectivity is also a critical factor. Fig. 4 presents the CO/N_2 pure-component isotherm selectivity of SAPO-34 and CuCl-loaded SAPO-34 adsorbents, calculating from the adsorption data from gas adsorption isotherms. As shown in Fig. 4, in the full investigated pressure range, the CO/N_2 adsorption selectivities of CuCl-loaded SAPO-34 adsorbents were greatly higher than that of the SAPO-34. The adsorption selectivities decreased gradually as the pressure increasing. Obviously, all of the CuCl-loaded SAPO-34 adsorbents exhibited preferential adsorption of CO over nitrogen, as a result of the stronger interaction between CuCl-loaded SAPO-34 adsorbents with CO via π-complexation. Table 2 summarized the CO adsorption capacities and CO/N_2 equilibrium selectivities of CuCl-loaded SAPO-34 and those reported in literatures. Cu(I) adsorbents have higher adsorption capacity than the conventional porous adsorbent. Scu(0.4) exhibited a relatively high CO adsorption capacities among those adsorbents.

3.3. Isosteric heat of adsorption of CO and N_2 on SCu(0.4)

Isosteric heat of adsorption is a crucial thermodynamic parameter to evaluate the interaction between the adsorbate and the adsorbent [25,26]. Pure CO and N_2 adsorption equilibrium isotherms at 298 K, 308 K and 318 K on SCu(0.4) were presented in Fig 5. It also showed that with the increase of the temperature, the adsorption amount of CO and N_2 both decreased, suggesting that the CO and N_2 adsorption of on SCu(0.4) were both exothermic processes. The isosteric heats adsorption of CO and N_2 were calculated by Clausius–Clapeyron equation using the adsorption equilibrium isotherms at different temperatures. The CO and N_2 adsorption isotherms were fitted by Langmuir–Freundlich model and fitting parameters were listed in Table 3. According to Clausius–Clapeyron equation, the isosteric heats of adsorption can be subsequently obtained the slopes of plots of ln$P$ as a function of $1/T$ at given adsorption amounts. At a certain adsorption amount, the pressures for different temperatures could be calculated from the fitted Langmuir–Freundlich equation. As presented in Fig. 6, the isosteric heat of CO adsorption was above 60 kJ/mol, suggesting the favorable interaction between CO and the CuCl-loaded SAPO-34 surface. It also obviously showed that the isosteric heat of CO adsorption on SCu(0.4) was remarkably higher than that of N_2, indicating that as a result of the π complexation bonds between Cu^+ ion and CO molecule, the interaction between CO and SCu(0.4) was much stronger than the physical interaction between N_2 and

Table 3. Langmuir-freundlich fitting parameters with average percent deviations for CO and N_2 adsorptions on SCu(0.4).

Temperature (K)	CO				N_2			
	q_m (mmol/g)	b (kPa^{-1})	n	R^2	q_m (mmol/g)	$b \times 10^{-3}$ (kPa^{-1})	n	R^2
298	23.69	0.0408	0.156	0.9946	4.84	0.338	0.944	0.9722
308	15.43	0.0587	0.123	0.9992	3.58	0.321	0.986	0.9693
318	14.08	0.0542	0.145	0.9985	4.42	0.175	0.957	0.9682

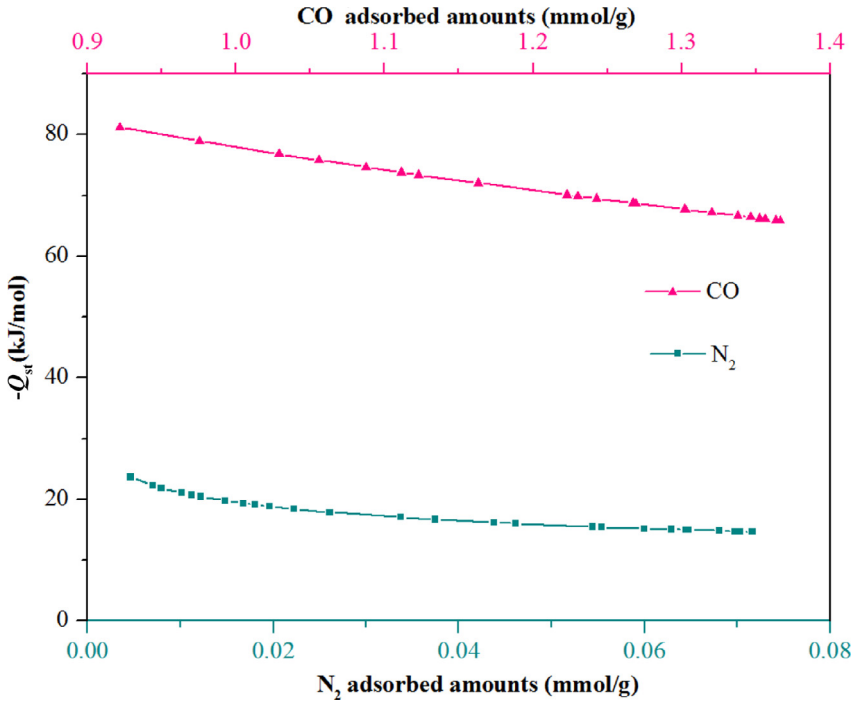

Fig. 6. Isosteric heat of adsorption for CO and N_2 on SCu(0.4).

SCu(0.4). The preferential adsorption capacity of CO on SCu(0.4) was much higher than that of N_2. Consequently, adsorbent SCu(0.4) achieved an efficient CO adsorption performance and high selectivity of CO/N_2.

4. Conclusions

In conclusion, CuCl-loaded SAPO-34 adsorbents have been successfully synthesized by monolayer dispersed method and exhibit efficient CO adsorption capacity and CO/N_2 selectivity. CuCl was highly dispersed on the surface of SAPO-34. With the increase loading amount of CuCl, the CO adsorption capacities of the resulting adsorbents were increased dramatically and further decreased as a result of the decrease porosity occupied by the CuCl. Sample SCu(0.4) exhibits a high CO adsorption amount of 1.84 mmol/g at 100 kPa and 298 K. The isosteric heats of CO and N_2 adsorption calculated by Clausius-Clapeyron equation indicated that the stronger interaction between the CuCl-loaded SAPO-34 adsorbent and CO than that of N_2.

Acknowledgments

The work was supported by the National Natural Science Foundation of China (No. 21802136).

References

[1] G. Zarca, I. Ortiz, A. Urtiaga, J. Memb. Sci. 438 (2013) 38–45, doi:10.1016/j.memsci.2013.03.025.
[2] G.S. Patil, S. Baruah, N.N. Dutta, Gas Sep. Purif. 5 (1991) 2–8, doi:10.1016/0950-4214(91)80040-C.
[3] J. Peng, S. Xian, J. Xiao, Y. Huang, Q. Xia, H. Wang, et al., Chem. Eng. J. 270 (2015) 282–289, doi:10.1016/j.cej.2015.01.126.
[4] T. Harlacher, M. Scholz, T. Melin, M. Wessling, Ind. Eng. Chem. Res. 51 (2012) 12463–12470, doi:10.1021/ie301485q.
[5] S. Feng, Y. Wu, J. Luo, Y. Wan, J. Energy Chem. 29 (2019) 31–39, doi:10.1016/j.jechem.2018.02.004.
[6] F. Gao, Y. Wang, S. Wang, Chem. Eng. J. 290 (2016) 418–427, doi:10.1016/j.cej.2016.01.054.
[7] F. Gao, Y. Wang, X. Wang, S. Wang, RSC Adv. 6 (2016) 34439–34446, doi:10.1039/C6RA03116A.
[8] Y. Yin, Z.-H. Wen, X.-Q. Liu, L. Shi, A.-H. Yuan, J. Porous Mater. 25 (2018) 1513–1519, doi:10.1007/s10934-018-0564-9.
[9] E.D. Bloch, M.R. Hudson, J.A. Mason, S. Chavan, V. Crocellà, J.D. Howe, et al., J. Am. Chem. Soc. 136 (2014) 10752–10761, doi:10.1021/ja505318p.
[10] B. Gao, M. Yang, Y. Qiao, J. Li, X. Xiang, P. Wu, et al., Catal. Sci. Technol. 6 (2016) 7569–7578, doi:10.1039/C6CY01461E.
[11] W. Dai, X. Wang, G. Wu, N. Guan, M. Hunger, L. Li, ACS Catal. 1 (2011) 292–299, doi:10.1021/cs200016u.
[12] D. Chen, K. Moljord, A. Holmen, Microporous Mesoporous Mater. 164 (2012) 239–250, doi:10.1016/j.micromeso.2012.06.046.
[13] D. Wang, L. Zhang, K. Kamasamudram, W.S. Epling, ACS Catal. 3 (2013) 871–881, doi:10.1021/cs300843k.
[14] J. Wang, T. Yu, X. Wang, G. Qi, J. Xue, M. Shen, et al., Appl Catal. B. 127 (2012) 137–147, doi:10.1016/j.apcatb.2012.08.016.
[15] S. Li, J.L. Falconer, R.D. Noble, J. Memb. Sci. 241 (2004) 121–135, doi:10.1016/j.memsci.2004.04.027.
[16] S.R. Venna, M.A. Carreon, Langmuir 27 (2011) 2888–2894, doi:10.1021/la105037n.
[17] Z. Zong, X. Feng, Y. Huang, Z. Song, R. Zhou, S.J. Zhou, et al., Microporous Mesoporous Mater. 224 (2016) 36–42, doi:10.1016/j.micromeso.2015.11.014.
[18] Y. Huang, L. Wang, Z. Song, S. Li, M. Yu, Angew. Chem. Int. Ed. 54 (2015) 10843–10847, doi:10.1002/anie.201503782.
[19] B.-U. Choi, D.-K. Choi, Y.-W. Lee, B.-K. Lee, S.-H. Kim, J. Chem. Eng. Data 48 (2003) 603–607, doi:10.1021/je020161d.

[20] Y. Yin, P. Tan, X.-.Q. Liu, J. Zhu, L.-.B. Sun, J. Mater. Chem. A 2 (2014) 3399–3406, doi:10.1039/C3TA14760F.
[21] J. Ma, L. Li, J. Ren, R. Li, Sep. Purif. Technol. 76 (2010) 89–93, doi:10.1016/j.seppur.2010.09.022.
[22] F.V.S. Lopes, C.A. Grande, A.M. Ribeiro, J.M. Loureiro, O. Evaggelos, V. Nikolakis, et al., Sep. Sci. Technol. 44 (2009) 1045–1073, doi:10.1080/01496390902729130.
[23] Y. Park, Y. Ju, D. Park, C.-.H. Lee, Chem. Eng. J. 292 (2016) 348–365, doi:10.1016/j.cej.2016.02.046.
[24] Q. Min Wang, D. Shen, M. Bülow, M. Ling Lau, S. Deng, F.R. Fitch, et al., Microporous Mesoporous Mater. 55 (2002) 217–230, doi:10.1016/S1387-1811(02)00405-5.
[25] S. Cavenati, C.A. Grande, A.E. Rodrigues, J. Chem. Eng. Data. 49 (2004) 1095–1101, doi:10.1021/je0498917.
[26] G. Srinivas, Y. Zhu, R. Piner, N. Skipper, M. Ellerby, R. Ruoff, Carbon 48 (2010) 630–635, doi:10.1016/j.carbon.2009.10.003.